J Solid State Electrochem (2010) 14:2275–2283
DOI 10.1007/s10008-010-1069-x

ORIGINAL PAPER

Voltammetric investigation and amperometric detection of the bisphosphonate drug sodium alendronate using a copper nanoparticles-modified electrode

Hossein Heli · F. Faramarzi · N. Sattarahmady

Received: 18 January 2010 / Revised: 22 March 2010 / Accepted: 30 March 2010 / Published online: 20 April 2010

Abstract The electrochemical behavior of sodium alendronate on copper microparticle- and copper nanoparticle-modified carbon paste electrodes was investigated. In the voltammograms recorded using microparticles, a single anodic oxidation peak appeared, while using nanoparticles, two anodic peaks appeared. The anodic currents were related to the electrocatalytic oxidation of alendronate via the active species of Cu(III). The catalytic rate constant for the electrocatalytic oxidation process and the diffusion coefficient of alendronate were obtained to be $1.57\times10^{3}\,cm^{3}\,mol^{-1}s^{-1}$ and $2.44\times10^{-6}\,cm^{2}s^{-1}$, respectively. A sensitive and time-saving detection procedure was developed for the analysis of alendronate, and the corresponding analytical parameters were reported. Alendronate was determined with a limit of detection of 11.26 μmol L^{-1} with a linear range of 50–6,330 μmol L^{-1}. The proposed amperometric method was applied to the analysis of commercial pharmaceutical tablets, and the results were in good agreement with the declared values.

Keywords Alendronate · Bisphosphonate drug · Copper · Nanoparticle · Electrocatalysis · Modified electrode

H. Heli (✉)
Laboratory of Analytical and Physical Electrochemistry,
Department of Chemistry, Islamic Azad University,
Fars Science and Research Branch,
P.O. Box 73715-181, Marvdasht, Iran
e-mail: hheli7@yahoo.com

H. Heli
Young Researchers Club, Islamic Azad University,
Fars Science and Research Branch,
Marvdasht, Iran

F. Faramarzi
Department of Chemistry, K. N. Toosi University of Technology,
Tehran, Iran

N. Sattarahmady
Department of Biochemistry,
Shiraz University of Medical Sciences,
Shiraz, Iran

Introduction

Bisphosphonates are synthetic analogs of pyrophosphate that prevent the dissolution of hydroxyl apatite, the principal bone mineral, and hence arresting bone loss. They use to treat or prevent postmenopausal osteoporosis and steroid-induced osteoporosis, osteitis deformans, bone metastasis, multiple myeloma, and other conditions that feature bone fragility [1, 2]. Alendronate (sodium [4-amino-1-hydroxy-1-(hydroxy-oxido-phosphoryl)-butyl]phosphonic acid trihydrate, Scheme 1) is an amino bisphosphonate compound and a potent antiresorptive agent used to treat abnormal bone turnover, such as Paget's disease, hypercalcemia of malignancy, metastatic bone disease, and osteoporosis [3].

Since alendronate lacks natural chromophore or fluorephore for photometric and flurometric detections, its determination is not simple. Determination of alendronate was performed by HPLC with flurometric [4] and electrophoretic [5] detections, which utilized the formation of chromophore complexes between alendronate and molybdenum [6], copper [7], and iron [8] species. The disadvantages of these methods are that they are not simple enough for the routine analysis and require sophisticated or expensive instruments. Meanwhile, alendronate was also analyzed using reverse-phase liquid chromatography [9], liquid chromatography coupled with mass spectrometry [10], ion chromatography with indirect UV detection [11] or conductivity detection [12], capillary electrophoresis [12], and

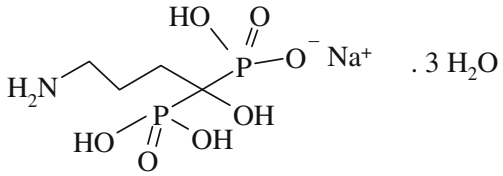

Scheme 1 The chemical structure of sodium alendronate

inductively coupled plasma mass spectrometry [13]. The latest edition of British Pharmacopeia [14] describes a liquid chromatography method with refractometric detection for the assay of sodium alendronate.

Nanostructured materials represent unique physicochemical properties differ largely from the large counterparts due to their limited size and a high density of corner or edge surface sites [15]. Nanostructures of metal oxides can adopt geometries not seen in the bulk state and show important variations in the oxygen/metal ratio. These nanomaterials bear oxygen vacancies not common in the bulk state enhancing the reactivity. On the other hand, nanoparticles can have an oxygen/metal ratio larger than observed for bulk oxides of a given metal [16]. Many types of nanostructured materials including nanotubes of carbon [17, 18], nanoparticles [19–21], and nanowires [22] have been employed in electrochemical analysis of drugs.

Electrochemistry is most suitable for investigating the redox properties of drugs that can give insight into its metabolic fate [23, 24]. Data obtained from electrochemical techniques are often correlated with molecular structures and pharmacological activities of drugs. Moreover, the electrochemical behaviors are valuable in elucidating some mechanisms of the drug action in vivo [25, 26]. In addition, electrochemistry has a well-defined role in drug analysis, and various electroanalytical methods are being used from time to time for this purpose. Electrochemical methods have attracted much attention because of quick response, high sensitivity, abilities to miniaturization, and analysis of drugs even in samples containing complex matrix. Most favorable property for modern electroanalytical methods is that excipients do not interfere. Hence, sample can be prepared simply by dissolution of pharmaceutical ingredient in a suitable solvent.

In the study described here, the electrocatalytic oxidation and determination of sodium alendronate in bulk as well as pharmaceutical forms on a copper nanoparticle-modified carbon paste electrode were investigated.

Experimental

Materials

Sodium alendronate was received as a gift from Arasto Pharmaceutical Chemicals Inc., Tehran, Iran. The alendronate tablets were obtained from a local drugstore. Copper microparticles with the diameter of <63 μm were obtained from Merck. Other chemicals were purchased from Merck or Sigma. All solutions were prepared with doubly distilled water. Copper nanoparticles were synthesized via solution phase reduction of copper(II) ions in the presence of a stabilizer to prevent the aggregation of the resultant copper nanoparticles according to the following procedure. Copper (II) sulfate (0.02 mol) was reduced with 30 mL 50% (*v*/*v*) hydrazine hydroxide solution in the presence of 1% (*w*/*v*) polyvilnylpyrrolidone. After 30 min, the resulting precipitate was centrifuged and washed thoroughly with distilled water. Then the product was dried in vacuum at room temperature. Brown powder of copper nanoparticles was obtained.

Apparatus

Electrochemical measurements were carried out in a conventional three-electrode cell powered by a μ-Autolab potentiostat/galvanostat, type III (The Netherlands). An Ag/AgCl, 3 mol L^{-1} KCl, a platinum disk (both from Azar electrode Co., Iran), and a carbon paste electrode (CPE) were used as the reference, counter, and working electrodes, respectively. The system was run by a PC using GPES 4.9 software.

Surface morphological studies were carried out using scanning electron microscopy (SEM), a X-30 Philips instrument. To obtain information about the morphology and size of particles, transmission electron microscopy (TEM) was also performed using a CEM 902A ZEISS instrument with an accelerating voltage of 80 kV. Samples were prepared by placing a drop of the particles, dispersed in acetone, on a carbon-covered copper grid (400 mesh), and evaporating the solvent.

Electrode preparation

Unmodified CPE (UCPE) was prepared by hand-mixing carbon powder and mineral oil with an 80/20% (*w*/*w*) ratio. The paste was carefully mixed and homogenized in an agate mortar for 20 min. The resulting paste before use was kept at room temperature in a desiccator. The paste was packed firmly into a cavity (3.6-mm diameter, geometric surface area of 0.1017 cm^2 and 0.5-mm depth) at the end of a Teflon tube. Electrical contact was established via a copper wire connected to the paste in the inner hole of the tube. The electrode surface was gently smoothed by rubbing on a piece of weighing paper just prior to use. This procedure was also used to regenerate the surface of the carbon paste electrodes. The copper microparticle- and copper nanoparticle-modified carbon paste electrodes (denoted as m-MCPE and n-MCPE, respectively) were

prepared by mixing carbon powder together with copper micro- or nanoparticles at different ratios in an agate mortar until a uniform paste was obtained. The percentage (*w*/*w*) of copper informed throughout the text corresponds to the final percentage relative to the total paste composition. Then mineral oil was added (20% *w*/*w*) and mixed thoroughly. The paste so obtained was packed into a 3-mm diameter cavity at the end of a Teflon tube, and the electrical contact was provided with a copper wire.

Procedures

Standard solutions of alendronate were prepared by dissolving accurate masses of the bulk drug in an appropriate volume of 100 mmol L^{-1} sodium hydroxide solution (which was also used as the running electrolyte throughout the work); the solutions were then stored in the dark at 4 °C. Additional dilute solutions were prepared daily by accurate dilution just before use.

In order to compare the catalytic currents generated using m-MCPE and n-MCPE, the effective surface areas of the electrodes were measured. Based on the mechanism of the reaction (vide infra), alendronate was oxidized on the active sites of copper generated at the electrode surfaces. Therefore, the catalytic currents must be normalized with respect to the total coverage area of copper active sites. To obtain such effective surface areas, the anodic charge passed for the oxidation of copper species was measured in alkaline solution for the modified electrodes; these values were related directly to the effective surface areas. Accordingly, the currents in the cyclic voltammograms were reported as current densities.

The calibration curves for alendronate in 100 mmol L^{-1} sodium hydroxide solution were measured by amperometric technique. Working potential of 610 mV was applied for the amperometric measurements, which the transient currents were allowed to decay to steady-state values.

For analysis of the drug tablets, the average mass of ten tablets was determined; then the tablets were finely powdered and homogenized in a mortar. An appropriate, accurately weighed amount of the homogenized powder was transferred into a beaker containing 100 mmol L^{-1} sodium hydroxide solution. The contents of the flask were sonicated for 30 min, and then the undissolved excipients were removed by filtration and diluted in a calibration flask to volume with the supporting electrolyte. Appropriate solutions were prepared by taking suitable aliquots of the clear filtrate and diluting them with 100 mmol L^{-1} sodium hydroxide solution. All studies/measurements were carried out at room temperature.

In order to study the accuracy and reproducibility of the proposed amperometry technique, recovery experiments were carried out using the standard addition method. In order to find out whether the excipients show any interference with the analysis, known amounts of pure alendronate were added to the pre-analyzed tablet formulation, and the mixtures were analyzed by the proposed methods. The recovery of alendronate was calculated using the corresponding regression equations of previously plotted calibration plots. The recovery results were determined based on five parallel analyses.

Results and discussion

Figure 1a shows a SEM image of the synthesized copper nanoparticles. Near-spherical particles with an average size of 35 nm are clearly observed, which some particles also aggregated. Figure 1b represents a TEM image of the copper nanoparticles which confirms the near-spherical shape with an average diameter of 35 nm. The particle size and morphology obtained from SEM and TEM images are the same.

Figure 2 shows cyclic voltammograms of 100 mmol L^{-1} sodium hydroxide solution recorded using UCPE (A), m-MCPE (B) and n-MCPE (C) in the absence (curves a) and presence (curves b) of 5.0 mmol L^{-1} alendronate in the

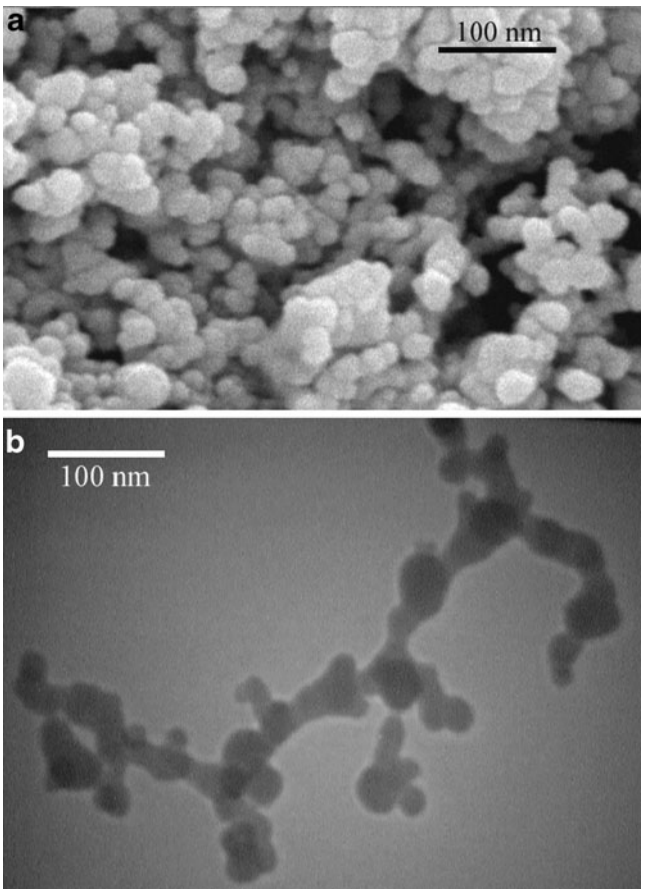

Fig. 1 SEM (**a**) and TEM (**b**) images of the copper nanoparticles

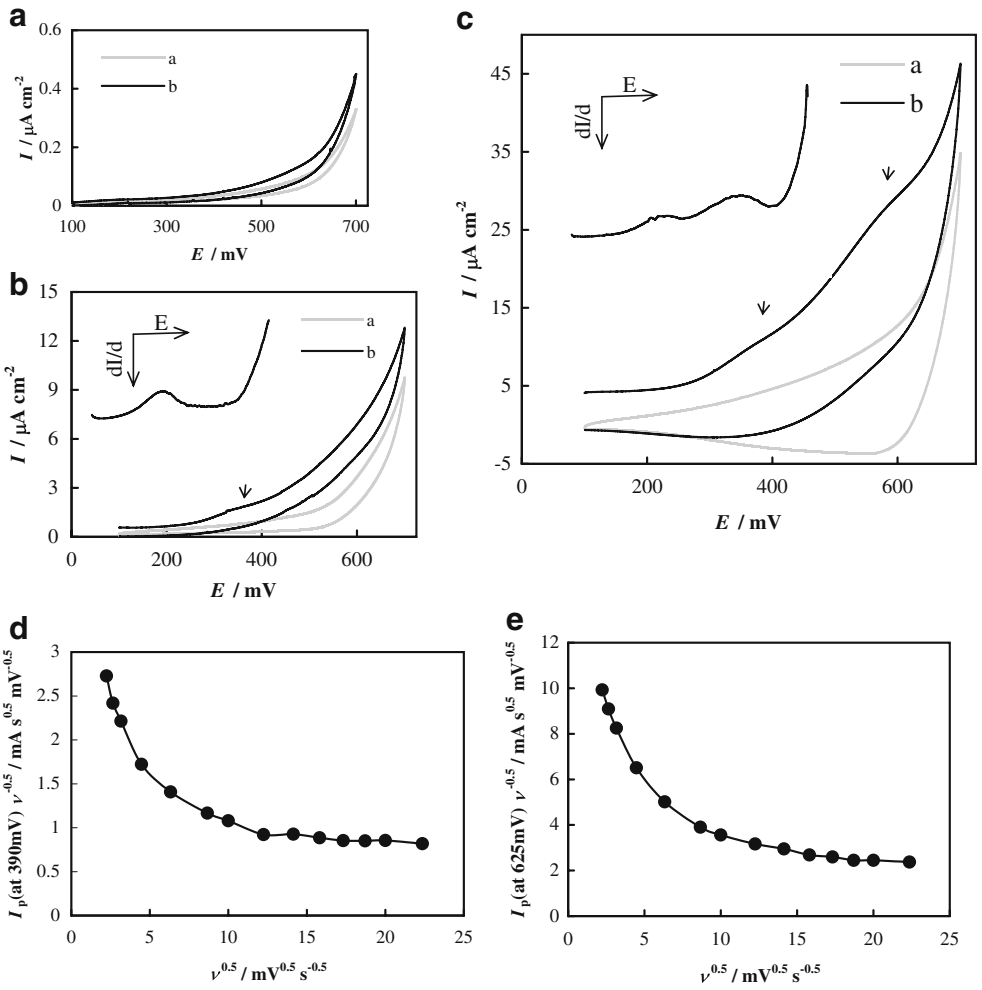

Fig. 2 Cyclic voltammograms recorded in the absence (*a*) and presence of 5 mmol L^{-1} alendronate (*b*) in 100 mmol L^{-1} sodium hydroxide solution using UCPE (**a**), m-MCPE (**b**), and n-MCPE (**c**). The potential sweep rate was 10 mV s^{-1}. The *insets* show the derivative voltammograms. Variation of peak currents with the square root of the potential sweep rate for the peaks located at 390 (**d**) and 625 mV (**e**)

potential range of 100 to 700 mV. Alendronate represents very weak oxidation signal on UCPE. This indicates the electroinactivity of alendronate on the carbon surface. However, alendronate was oxidized on both m-MCPE and n-MCPE surface. On the m-MCPE surface, alendronate was oxidized via a single anodic peak located at around 380 mV, and on the n-MCPE, surface alendronate was oxidized via two anodic peaks located at 390 and 625 mV (the peaks are indicated by arrows in the voltammograms). These were followed by a decrease in the cathodic peak current in the reverse sweep. The appearance of one and two peaks in the voltammograms and the one- and two-step electrooxidation reaction of alendronate on the m-MCPE and n-MCPE surfaces, respectively, were further confirmed by representation of derivative voltammograms (Fig. 2, insets). In addition, the anodic current densities related to the electrooxidation of the drug on the n-MCPE surface were higher compared to m-MCPE at both potentials of 390 and 625 mV. It can be related to the nanosize effect of the copper nanoparticles which represented higher reactivity compared to those of microparticles, because the currents were normalized for the effective surface areas of both electrodes (vide supra). Therefore, the electrooxidation of alendronate was performed by the nanoparticles with a higher rate. This is the kinetic enhancement effect of the nanomaterials [27–29].

The electrochemical behavior of copper in alkaline solutions has been extensively investigated [30–33]. In the entire range of potential window of aqueous electrolytes, different copper species are created, and the Cu(II)/Cu(III) redox transition performs at the anodic edge of the voltammograms in alkaline solutions [30–33]. Regarding the nature of Cu(III) entity, species ranging from CuOOH to Cu(III) radical have been proposed [34, 35]. On the other hand, Cu (III) species can oxidize organic and biological compounds by chemical reaction(s) between these materials and Cu(III) species via a redox mediation electron transfer process (mediated electrocatalytic reaction, EC' mechanism) at the anodic edge of the voltammograms in alkaline solutions [30, 34–36]. Based on this literature review, it can be deduced that alendronate was oxidized on both m-MCPE and n-MCPE surfaces via the active Cu(III) species. Copper species are immobilized on the electrode surfaces, and the one with a higher valence oxidizes alendronate via

chemical reactions. It is followed by generation of lower valence species. Therefore, the electrode reactions may proceed via a mechanism involving a rate-limiting step, in which product species are formed upon chemical reactions of alendronate with Cu(III) species, and regeneration of the surface occurs through chemical redox reactions. The participation of Cu(III) species as the catalyst of the electrooxidation reaction and the dominated EC' mechanism are further supported by the variation of current function (peak current divided by the square root of the potential sweep rate) with respect to the square root of the potential sweep rate. The data for these variations (for both peaks) which were obtained from cyclic voltammograms recorded at different potential sweep rates (not shown) are represented in Fig. 2d, e. In this figure, current function is smoothly decreased upon increasing the potential sweep rate confirming the electrocatalytic nature of the electrooxidation process. Based on the represented explanation and the results, the following mechanism can be proposed for the mediated oxidation of the drugs on the n-MCPE surface. The redox transition of the copper species:

$$\mathrm{Cu(II)} \rightleftarrows \mathrm{Cu(III)} + e \tag{1}$$

is followed by the oxidation of alendronate on the n-MCPE surface in two steps via the following reactions:

$$\mathrm{Cu(III)} + \mathrm{Alendronate} \xrightarrow{k_{\mathrm{cat1}}} \mathrm{Intermediate/Product\ 1} + \mathrm{Cu(II)} \tag{2}$$

$$\mathrm{Cu(III)} + \mathrm{Alendronate/Intermediate} \xrightarrow{k_{\mathrm{cat2}}} \mathrm{Product\ 2} + \mathrm{Cu(II)} \tag{3}$$

Scheme 2 The proposed reactions for the electrocatalytic oxidation of alendronate

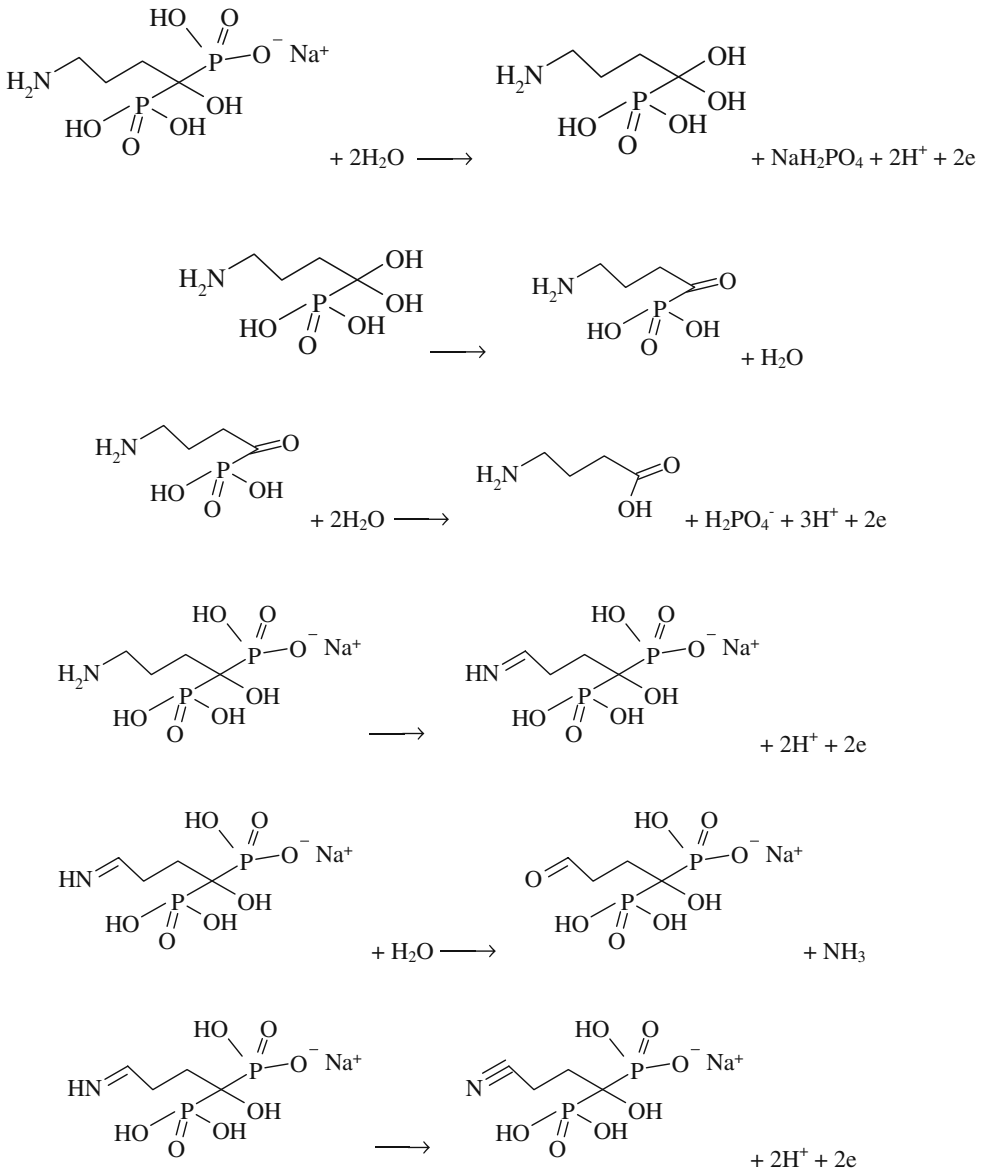

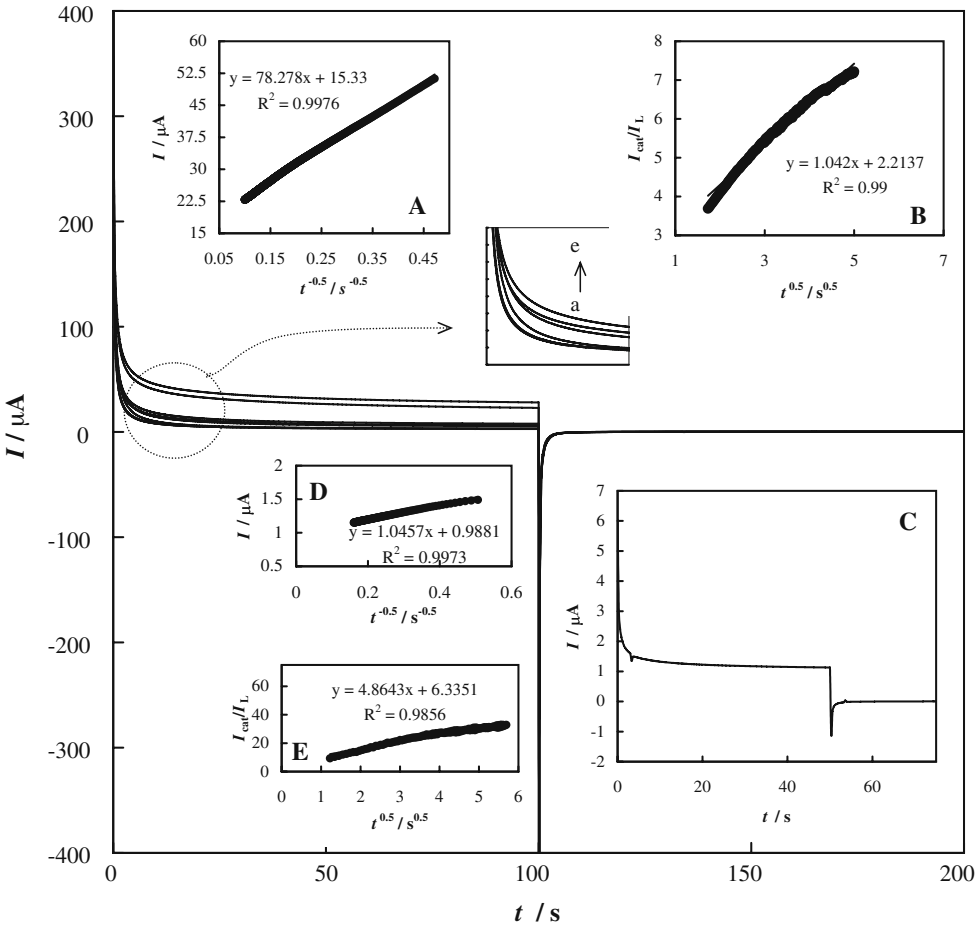

Fig. 3 *Main panel*: Double-step chronoamperograms of n-MCPE in 100 mmol L^{-1} sodium hydroxide solution with different concentrations of alendronate of *a* 0, *b* 0.05, *c* 0.5, *d* 3.0, and *e* 5.0 mmol L^{-1}. Potential steps were 420 and 100 mV, respectively. *Inset A*: Dependency of transient current on $t^{-0.5}$ related to curve *e* in main panel. *Inset B*: Dependence of I_{cat}/I_d on $t^{0.5}$ related to curve *e* in main panel. *Inset C*: Double-step chronoamperogram of n-MCPE in 100 mmol L^{-1} sodium hydroxide solution with 5.0 mmol L^{-1} alendronate. Potential steps were 650 and 130 mV, respectively. *Inset D*: Dependency of transient current on $t^{-0.5}$ related to chronoamperogram represented in *inset C*. *Inset E*: Dependence of I_{cat}/I_d on $t^{0.5}$ related to chronoamperogram represented in *inset C*

The proposition of a two-step reaction for the electrocatalytic oxidation of alendronate on the n-MCPE surface (reactions 2 and 3) is based on the appearance of two anodic peaks in the corresponding voltammogram (Fig. 2c, curve b).

Higher catalytic rate of the electrooxidation reaction can be related to nanometer dimension of copper nanoparticles. The nanoparticles are stably distributed on the electrode surface which is a fully and easily accessible alendronate and, consequently, can be readily and completely used as electrochemical reaction units. Moreover, nanoparticles are often irregularly shaped objects, and hence, there are some defect sites, such as steps that separate planar atomic terraces or kinks where a step advances or recedes, exposing corner or edge atoms on a plane. The enhancement of the reactivity of these defective sites can be so large that their presence determines to a very large extent the catalytic activity of nanoparticles.

For the mechanism of the electrooxidation reaction of alendronate, it can be proposed the oxidation of one functional group in multiple steps and/or simultaneous oxidation of different functional groups present in the chemical structure of alendronate. Herein, as an alcohol analog, alendronate cannot be oxidized because it is a third-

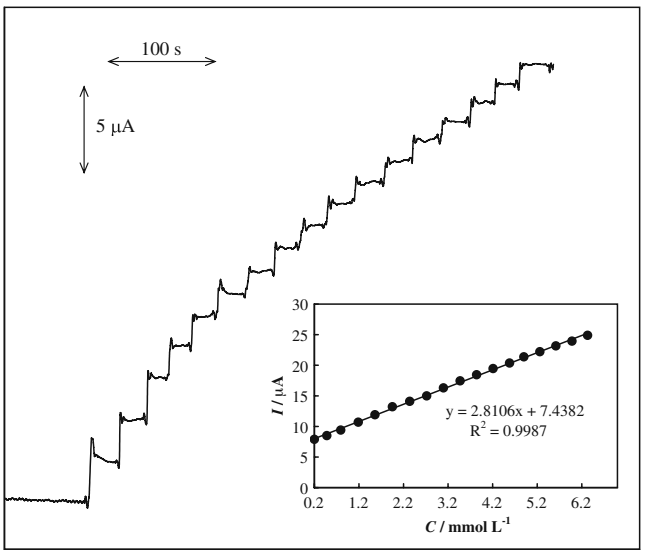

Fig. 4 *Main panel*: Current signal as a function of time in 100 mmol L^{-1} sodium hydroxide solution during repetitive injections of alendronate using n-MCPE. Applied potential was 610 mV. *Inset*: Dependency of the transient current on alendronate concentration using n-MCPE

Table 1 The determined parameters for calibration curve of the drug and accuracy and precision (n=3) for electrocatalytic oxidation of alendronate on n-MCPE

Linear range (μmol L^{-1})	50–6330
Slope (mA $Lmol^{-1}$)	2.8±0.1
Intercept (μA)	7.4±0.3
LOD (μmol L^{-1})	11.26
LOQ (μmol L^{-1})	37.53

type alcohol. First- and second-type alcohols can be oxidized to the corresponding aldehydes or ketones [37], but third-type ones cannot. As a first type amine analog, alendronate can be oxidized to the corresponding imine, nitril, and/or aldehyde analogs [36–38]. Alendronate is also oxidized via the C–P bond breaking. The proposed reaction mechanism is shown in Scheme 2.

In order to evaluate the reaction kinetics, the oxidation of alendronate on n-MCPE was investigated by chronoamperometry. Figure 3, main panel, shows double-step chronoamperograms which recorded in the absence (curve a) and presence (curves b–e) of different concentrations of alendronate using the potential steps of 420 and 100 mV, respectively. In Fig. 3, inset C, a typical double-step chronoamperogram recorded in the presence of 0.53 mmol L^{-1} alendronate using applied potential steps of 650 and 130 mV respectively, is also shown. As can be seen, the transient currents at two applied potentials of 420 and 650 mV decayed with time in a Cotrellian manner (Fig. 3, insets A and D). This indicates that the two steps of the electrocatalytic oxidation of alendronate on n-MCPE were controlled by diffusion in the bulk of solution. Therefore, alendronate is electrocatalytically oxidized on nanoparticles of copper via two diffusion-controlled steps. By using the slope of the line represented in Fig. 3, inset A, the diffusion coefficient of alendronate can be obtained using the Cottrell equation:

$$I = nFAD^{1/2}C\pi^{-1/2}\,t^{-1/2} \tag{6}$$

where D is the diffusion coefficient, A is the electrode surface area, and C is the bulk concentration. The mean value of the diffusion coefficient for alendronate was found to be $2.44 \times 10^{-6}\,cm^2 s^{-1}$. For the calculation of the diffusion coefficient, the chronoamperogram recorded at 420 mV which corresponds to the first step of electrocatalytic oxidation of alendronate was used. This is due to the uncertainty of the concentration for the second step of the reaction.

Chronoamperometry can also be used for the evaluation of the catalytic rate constant according to the following equation [39]:

$$I_{cat}/I_L = \lambda^{1/2}\left[\pi^{1/2}\mathrm{erf}\left(\lambda^{1/2}\right) + \exp(-\lambda)/\lambda^{1/2}\right] \tag{7}$$

where I_{cat} and I_L are the currents in the presence and absence of alendronate, respectively, and $\lambda = k_{cat}Ct$ is the argument of the error function. k_{cat} is the catalytic rate constant, and t is the elapsed time. In the cases where $\lambda > 1.5$, $\mathrm{erf}(\lambda^{1/2})$ is almost equal to unity, and the above equation can be reduced to:

$$I_{cat}/I_L = \lambda^{1/2}\,\pi^{1/2} = \pi^{1/2}(k_{cat}Ct)^{1/2} \tag{8}$$

From the slope of the I_{cat}/I_L vs. $t^{1/2}$ plot, presented in Fig. 3, inset B, the mean value of k_{cat} for the first step of alendronate oxidation was obtained as $1.57 \times 10^3\,cm^3\,mol^{-1}s^{-1}$. Using similar approach with the linear plot represented in Fig. 3, inset E, the value of catalytic rate constant for the second step of the oxidation reaction multiplied by the concentration was obtained as $C \times k_{cat2} = 5.6\,s^{-1}$.

In order to develop a simple and time-saving method for the analysis of alendronate in pure form as well as pharmaceutical formulations, the technique of hydrodynamic amperometry was employed. Typical amperometric signals obtained during successive increments of alendronate to a 100 mmol L^{-1} sodium hydroxide solution using n-MCPE are depicted in Fig. 4. Gentle stirring for a few seconds was needed to promote solution homogenization after each injection. The electrode response was quite rapid

Table 2 Determination and recovery of alendronate in pharmaceutical forms

Sample type	Amount labeled (mg)	Amount added (mg)	Amount found (mg)	Recovery (%)	Relative standard deviation (RSD) (%) for n=3	Bias (%)
Tablet sample 1	70	–	70.4	100.6	4.7	0.6
Tablet sample 1	–	70	67.7	96.7	4.3	−3.3
Tablet sample 1	–	70	65.9	94.14	4.6	−5.8
Tablet sample 2	70	–	72.0	102.8	2.6	2.8
Tablet sample 2	–	70	71.9	102.6	1.2	2.6
Tablet sample 2	–	70	68.8	98.3	2.9	−2
Tablet sample 3	70	–	70.5	100.7	1.5	0.7
Tablet sample 3	–	70	68.2	97.4	1.6	−2.5
Tablet sample 3	–	70	66.8	95.4	1.8	−4.5

and proportional to the alendronate concentration. The corresponding calibration curve for the amperometric signals is shown in Fig. 4, inset. The limits of detection (LOD) and quantitation (LOQ) of the procedure were calculated according to the 3 SD/m and 10 SD/m criteria, respectively, where SD is the standard deviation of the intercept and m is the slope of the calibration curve [40]. The determined parameters for calibration curve of drug, accuracy and precision, LOD and LOQ, and the slope of calibration curve are reported in Table 1. The value of LOD obtained here is comparable with some other previously reported [41] and is lower than the other [9].

The applicability of the proposed amperometric method for the sample dosage form was examined by analyzing the tablets. It was found that the amounts of drug determined using this method are in good agreement with the reported values. The values of experimentally determined drugs and declared values in tablets are reported in Table 2.

In order to evaluate the accuracy of this method and to know whether the excipients in pharmaceutical dosage forms show any interference with the analysis, the proposed amperometric method was checked by recovery experiments using the standard addition method. After addition of known amounts of pure drug to various pre-analyzed formulations of alendronate, the mixtures were analyzed by the proposed method. The recovery of alendronate was calculated using the corresponding regression equation of previously plotted calibration plot. The results of recovery experiments using the developed assay procedure are presented in Table 2. The results indicate the absence of interference from commonly encountered pharmaceutical excipients used in the selected formulations. Therefore, the method can be applied to the determination of alendronate in pharmaceutical forms without any interference from inactive ingredients.

Selectivity of the amperometric procedure for the assay of alendronate was examined in the presence of some common excipients in the same ratios usually used in pharmaceutical preparations (for example, gelatin, talc, starch, and magnesium stearate). The results showed no significant interference from excipients of tablets of alendronate. Therefore, the procedure was able to assay alendronate in the presence of excipients, and hence, it can be considered selective.

Conclusion

Carbon paste electrodes modified with microparticles and nanoparticles of copper were employed for the study of the electrocatalytic oxidation and determination of alendronate. Alendronate was oxidized on copper-based electrodes via mediation of Cu(III) active species. m-MCPE represented a single anodic peak in the voltammograms, while n-MCPE generated two anodic peaks with the higher corresponding currents. The current enhancement of the electrocatalytic oxidation of alendronate using the nanoparticles was related to the acceleration of the electrooxidation process by nanosize effect of copper nanoparticles. An amperometric procedure was successfully applied using n-MCPE for the quantification of the alendronate with high sensitivity in bulk and of pharmaceutical samples.

Acknowledgments The financial support of the Research Councils of Islamic Azad University and the K. N. Toosi University of Technology are gratefully acknowledged.

References

1. Fleisch H (1983) Bone and mineral research, annual 1. Excerpta Medica, Amsterdam
2. Fleisch H (1995) Bisphosphonates in bone disease, from the laboratory to the patient. Parthenon, New York
3. Sleeboom HP, Bijovet OLM, Van Osterom AT, Gleed JH, Oriordan JLH (1983) Lancet 2:239
4. Ptacek P, Klima J, Macek J (2002) J Chromatogr, B 767:111
5. Kline WF, Matuszowski BK (1992) J Chromatogr, B 583:183
6. Daley-Yates PT, Gifford LA, Hoggart CR (1989) J Chromatogr, B 490:329
7. Ostovic D, Stelmach C, Hulshizer B (1993) Pharm Res 10:470
8. Kuljanin J, Jankovic I, Nedeljkovic J, Prstojevic D, Marinkovic V (2002) J Pharm Biomed Anal 28:1215
9. Xie Z, Jiang Y, Zhang D (2006) J Chromatogr, A 1104:173
10. Qin XZ, Tsaie W, Sakuma T, Ip DP (1994) J Chromatogr, A 686:205
11. Al Deeb SK, Hamdan II, Al Najjar SM (2004) Talanta 64:695
12. Tsai EW, Ip DP, Brooks MA (1992) J Chromatogr, A 596:217
13. Kovacevic M, Gartner A, Novic M (2004) J Chromatogr, A 1039:77
14. British Pharmacopoeia (2007) System Simulation Ltd., London, v1.16c
15. Jortner J, Rao CNR (2002) Pure Appl Chem 74:1491
16. Fernandez-Garcia M, Martinez-Arias A, Hanson J, Rodriguez J (2004) Chem Rev 104:4063
17. Yadegari H, Jabbari A, Heli H, Moosavi-Movahedi AA, Karimian K, Khodadadi A (2008) Electrochim Acta 53:2907
18. Majdi S, Jabbari A, Heli H, Yadegari H, Moosavi-Movahedi AA, Haghgoo S (2009) J Solid State Electrochem 13:407
19. Houshmand M, Jabbari A, Heli H, Hajjizadeh M, Moosavi-Movahedi AA (2008) J Solid State Electrochem 12:1117
20. Heli H, Jabbari A, Moosavi-Movahedi AA, Tabeshnia M (2009) Chem Anal (Warsaw) 54:619
21. Heli H, Jabbari A, Majdi S, Mahjoub M, Moosavi-Movahedi AA, Sheibani S (2009) J Solid State Electrochem 13:1951
22. Liu L, Junfeng J (2006) Anal Biochem 354:22
23. Wang J (1988) Electroanalytical techniques in clinical chemistry and laboratory medicine. Wiley-VCH, New York
24. Kissinger PT, Heineman WR (1996) Laboratory techniques in electroanalytical chemistry. Marcel Dekker, New York
25. Permentier HP, Bruins AP (2008) Mini Rev Med Chem 8:46
26. Lin AMY, Chai CY (1998) Neurosci Res 31:171
27. Heli H, Jabbari A, Zarghan M, Moosavi-Movahedi AA (2009) Sens Actuators, B 140:245
28. Heli H, Majdi S, Sattarahmady N (2010) Sens Actuators, B 145:185

29. Heli H, Majdi S, Jabbari A, Sattarahmady N, Moosavi-Movahedi AA (2010) J Solid State Electrochem (in press)
30. Marioli JM, Kuwana T (1992) Electrochim Acta 37:1187
31. Burke LD, Ahern MJG, Ryan TG (1990) J Electrochem Soc 137:553
32. Shams El Din AM, Abd El Wahab FM (1964) Electrochim Acta 9:113
33. Brisard GM, Rudnicki JD, McLarnon F, Cairns EJ (1995) Electrochim Acta 40:859
34. Meyerstein D, Hawkridge FM, Kuwana T (1972) J Electroanal Chem 40:377
35. Fleischmann M, Korinek K, Pletcher D (1972) J Chem Soc, Perkin Trans 10:1396
36. Hampson NA, Lee JB, Macdonald KI (1972) J Electroanal Chem 34:91
37. Steckham E (1991) In: Lund H, Hammerich O (eds) Organic electrochemistry. Marcel Dekker, New York, Chapter 15
38. Fleischmann M, Korinek K, Pletcher D (1971) J Electroanal Chem 31:39
39. Bard AJ, Faulkner LR (2001) Electrochemical methods. Wiley, New York
40. Miller JC, Miller JN (1994) Statistics for analytical chemistry, 4th edn. Ellis-Howood, New York
41. Kuljanin J, Jankovic I, Nedeljkovic J, Prstojevic D, Marinkovic V (2002) J Pharmaceut Biomed Anal 28:1215